P.C. de Vries, E. Joffrin, M. Brix, C.D. Challis, K. Crombé, B. Esposito,
N.C. Hawkes, C. Giroud, J. Hobirk, J. Lönnroth, P. Mantica, D. Strintzi,
T. Tala, I. Voitsekhovitch and JET EFDA contributors

Internal Transport Barrier Dynamics with Plasma Rotation in JET

Internal Transport Barrier Dynamics with Plasma Rotation in JET

P.C. de Vries[1], E. Joffrin[2,3], M. Brix[1], C.D. Challis[1], K. Crombé[4], B. Esposito[5], N.C. Hawkes[1], C. Giroud[1], J. Hobirk[6], J. Lönnroth[7], P. Mantica[8], D. Strintzi[9], T. Tala[10], I. Voitsekhovitch[1] and JET EFDA contributors*

JET-EFDA, Culham Science Centre, OX14 3DB, Abingdon, UK

[1]*EURATOM/UKAEA Fusion Association, Culham Science Centre, Abingdon, OX14 3DB, UK.*
[2]*JET-EFDA-CSU, Culham Science Centre, Abingdon, Oxfordshire, OX14 3DB, UK.*
[3]*Association Euratom-CEA, Cadarache, F-13108, France.*
[4]*Department of Applied Physics, Ghent University, Rozier 44, 9000 Gent Belgium*
[5]*Associazione Euratom-ENEA sulla Fusione, Via E. Fermi 45, 00044 Frascati, Roma, Italy.*
[6]*Max-Planck-Institut f r Plasmaphysik, Euraton Association, 85748, Garching, Germany.*
[7]*Association Euratom-Tekes, Helsinki University of Technology, P.O. Box 4100, Finland.*
[8]*Istituto di Fisica del Plasma, EURATOM/ENEA-CNR Association, Milano, Italy.*
[9]*National Technical University of Athens, EURATOM Association, GR-15773, Athens, Greece.*
[10]*Association Euratom-Tekes, VTT, PO Box 1000, 02044 VTT, Finland.*
* See annex of F. Romanelli et al, "Overview of JET Results",
(Proc. 22 nd IAEA Fusion Energy Conference, Geneva, Switzerland (2008)).

ABSTRACT.

At JET the dynamics of Internal Transport Barriers (ITBs) has been explored by trying to decouple the effects of heating on one hand and torque on the other with the ultimate objective of identifying the minimum torque required for the formation of transport barriers. The experiments shed light on the physics behind the initial trigger for ITBs, which often shows to be linked to the shape of the q profile and magnetic shear, while the further development was influenced by the strength of the rotational shear. In discharges with a small amount of rotational shear ITBs were triggered, which suggest that the overall rotational shear is not the dominant factor in the triggering process. However, the subsequent growth of the barrier was limited if the rotational shear was too low at the time of triggering. This growth phase may be highly non-linear, with several possible positive feedback loops, such as the increases of the toroidal and poloidal component of the rotational shear caused by the ITB itself.

1. INTRODUCTION

Advanced Tokamak scenarios are proposed to provide the conditions for steady-state operations of ITER [1, 2, 3, 4]. This scenario aims to operate at high pressure ($\beta_N \sim 3$) and modest plasma current ($I_p \sim 9MA$, $q_{95} \sim 5$) with a large bootstrap current providing a non-inductive self-generated current. Internal Transport Barriers (ITBs) are considered as a candidate for enhancing the confinement and reaching these higher pressures.

Various physical mechanisms are thought to enable the formation of transport barriers in plasmas by causing a local suppression of turbulence. Because, these mechanisms may not necessarily act independently, the whole process may be an interplay of more than one mechanism, making it difficult to identify the physics roots behind ITB formation. Nevertheless, studies identified two factors that play a crucial role: magnetic and rotational shear [5, 6].

It was found for example that ITBs form more easily in plasmas that have a particular current density profile and safety factor, q, profile, such that there exists a region of low or even negative magnetic shear, $r \cdot q'/q$ [7], furthermore, the initial formation or triggering of ITBs, is often closely linked to detailed characteristics of the q profile [8]. The role of rotational shear has been pointed out in experiments in JT-60U and TFTR which applied balance Neutral Beam Injection (NBI) in order to create low torque plasmas with ITBs [9, 10]. At JET internal transport barriers are usually formed in discharges with predominant NBI and this system provides a large toroidal torque and consequently a large rotational shear. Studies have shown the effect of rotational shear on ITBs in JET discharges with small but positive magnetic shear [11]. Experiments to produce ITBs with low torque have been performed previously by simply increasing the fraction of Ion Cyclotron Resonance Heating (ICRH). However, the variety of differences between the NBI and ICRH, such as the power deposition profiles, ion and electron heating fraction or current drive characteristics, adds to the difficulty in interpreting the experimental results [12].

In next step devices such as ITER the rotational shear induced by the NBI is not expected to be

as high as in the present devices. In this context, the understanding of the ITB dynamics has been explored at JET by trying to decouple the effects of heating on one hand and torque on the other with the ultimate objective of identifying the minimum rotational shear required for the formation and development of broad ITB as required for the steady state scenario. Decoupling these two effects should also assist in separating the physics of the initial triggering of the barrier and its further development.

JET has developed several original experiments to study these aspects. First of all, JET has the unique ability to modify the amplitude of the toroidal magnetic field ripple. The Toroidal Field (TF) ripple has been shown to affect the toroidal rotation and tuning the ripple may alter the shape of the rotation profile [13]. In a second set of experiments, a specific ICRH heating scheme has been used, which couples to ^{3}He minority, providing ion heating close to the plasma centre with no excitation of H minority or D majority species. The toroidal momentum deposited in the plasma can be changed by varying the mixture of ICRH and NBI heating whilst keeping the total power to the ions and ion heat flux constant [14]. This paper will describe and compare both experiments in section 2, showing the effect of plasma rotation and rotational shear on transport barriers. The focus is on ion barriers formed in plasmas with reversed central magnetic shear. Section 3 deals with the details of the growth phase of the transport barriers in both experiments and the role played by toroidal and also poloidal rotational shear on this process, after which the conclusions will be summarized in the last section.

2. ITB EXPERIMENTS AT JET

The internal transport barriers studied in the paper are formed in plasmas with reversed central magnetic shear. Early heating is applied, during the current ramp-up phase, combined with a prelude of Lower Hybrid Current Drive (LHCD). This produces a hollow q profile with reversed shear as can be seen in the q profile contours in figure 1c. These profiles have been obtained using equilibrium reconstructions constrained by Motional Stark Effect (MSE) polarimetry and pressure profile data. Within the uncertainties of the measurement one finds that the minimum q value, q_{min}, in the plasma is around or just below 2. So-called grand-cascades of AlfvÈn modes [8, 15] are usually triggered around this time which gives an accurate time of the appearance of the integer q surface, which in these plasmas often lead to the subsequent formation of an ITB.

The presence of ITBs can be deduced from the local steepening of the temperature gradient. The temperature gradient can be expressed by a normalised value, $\rho^*_T \equiv \rho_s/L_T$, i.e. the ratio of the ion Larmor radius at the sound speed and the temperature gradient length [16]. A transport barrier is said to be present if the ρ^*_T value exceeds the empirical threshold of the $\rho^*_T > \rho^{*crit}_T = 0.014$ [16]. In figure 1c the contours of the ion ρ^*_T are shown as a function of time and major radius. Soon after the switch on of NBI and ICRH, signs of a temperature profile steepening can be found. These are remnants of a barrier that formed during the LHCD prelude phase, located in the negative shear region, persisting briefly in the main experimental phase. At approximately the same time (t~5s)

another ITB forms (Indicated by the dashed line in figure 1c). This coincides with an increase in the central ion temperature as shown in figure 1b. A weak outer and inner transport barrier can be seen, the latter moving radially inward. This signature, in the ρ^*_T contours, seems to be linked to the appearance of a rational q-surface in the plasma, and indeed a grand-cascade appears in 69670 quickly after the ITB trigger. This feature, identical to those observed in ref. [8, 17], cannot be predicted by transport models since usually no role is given to rational surfaces. On the other hand rarefaction of rational flux surfaces, i.e. the rarity of these surfaces, has been proposed to influence transport [18, 19]. It has been shown that zonal-flow structures can occur due to the gap in low order rational surfaces near integer q surfaces, causing modifications to the temperature profiles just after the minimum q drops below an integer value [20]. This would predict a steepening of the temperature profile to appear on both sides of the minimum q, after the q = 2 surface appears in the plasma, which is very similar to what is observed in this discharge.

In these experiments this ITB triggering scenario remained unchanged, although the rotation properties were altered by tuning respectively the toroidal field ripple or increasing the ICRH to NBI power fraction.

2.1. EXPERIMENTS USING TF RIPPLE

Standard operations at JET are carried out with a set of 32 toroidal field coils, all carrying equal current. At JET it is possible to vary the toroidal field ripple amplitude by independently powering the 16 odd and 16 even-numbered coils [21]. The imbalance current between the two coil sets can be changed in a controlled way increasing the TF ripple amplitude, δ_{BT}, defined as the relative amplitude of the magnetic field variation: $\delta_{BT} = (B_{max}-B_{min})/(B_{max} + B_{min})$. The values quoted in the remainder of this paper, are the maximum ripple in the plasma which is usually found at the separatrix near the outboard mid-plane. For standard JET operations (with 32 coils) the TF ripple is $d_{BT}=0.08\%$.

The TF ripple breaks the axi-symmetry of the magnetic field and enhances particle losses, in particular energetic ions such as alpha particles created in fusion reactions and those injected by NB or accelerated by ICRH. These non-ambipolar ion losses will have a significant impact on the plasma rotation. The return current due to the ion losses, induces a $j \times B$ torque in counter-current direction that counteracts the NBI torque on the plasma, which is in co-current direction at JET. Increased levels of TF ripple have been found to reduce the plasma rotation in JET and even created regions where the plasma rotated in counter current direction [13]. Since the torque deposition profile of the NBI and that induced by the TF ripple are not the same, also rotation profile shape is modified. TF ripple has been used as a tool to tune the plasma rotation and rotational shear in typical scenarios that formed ITBs, utilizing optimised low and reversed central magnetic shear [22]. These specific experiments used a toroidal magnetic field, B = 2.2T, and plasma current, I_p = 1.8MA (q_{95} = 4.2) and used a plasma configuration with an elongation of κ = 1.74 and a low triangularity of δ = 0.22.

The example shown in figure 1, was done with a standard TF ripple amplitude of $\delta_{BT}=0.08\%$. In figure 2, this was repeated, albeit with a larger TF ripple of δ_{BT} = 0.08% and 1.0%, respectively.

Since the TF ripple induces losses of NB injected particles, the applied auxiliary power for the discharge with the highest TF ripple (69668) is slightly higher, to correct for the ripple losses. The power loss fraction and the total absorbed power have been calculated using the JAEA Orbit Following Monte Carlo (OFMC) code [23]. For these scenarios it was found that typically 17% of the NBI power is lost with a TF ripple of $\delta_{BT} = 1.0\%$. For standard JET operations with $d_{BT}=0.08\%$ these losses are negligible. Although the absorbed power is kept constant ($P_{abs} = 14.5MW$), the plasma rotation in both pulses was found to be significantly different. The main resulting difference between the two examples is the much lower rotational shear in the case with the higher TF ripple (69668) as will be discussed in detail later.

Grand-cascades of Alfvén modes have been seen in discharge 69670 at $t = 3.8s$ and another one at $t{\sim}5s$, while for 69668 these modes are only seen at $t = 3.7s$. The integer q values that appear in the plasma and trigger these modes may be identified by $q = 3$ and $q = 2$ for the two times in 69670. Although ITBs are found to be triggered in both discharges, there is a striking difference in the subsequent development. In discharge 69668 the value of ρ^*_T never exceeds 0.022, as shown in figure 2c, while in 69670 the outer barrier grows and reaches values of $\rho^*_T = 0.065$ (see figure 1c). Because such strong barriers with large pressure gradients have been seen to trigger internal kink-modes and subsequent disruptions, the NBI power in this discharge is stepped-down prematurely in order to prevent this. The strength of the barrier is sufficient to significantly increase the central ion temperature and normalised b, b_N, no such effect was seen in discharge 69668.

As pointed out before, the difference between these two discharges is the TF ripple amplitude which altered the toroidal rotation profile and rotational shear at the time of ITB triggering, as shown in figure 3. This has been explored further by carrying out a scan in TF ripple amplitude, keeping the scenario unchanged, applying the same level of absorbed power $P_{abs} = 14.5MW$. ITB trigger events have been found in all four cases. However, as shown in figure 4, the peak performance, expressed as b_N, clearly decreases with TF ripple amplitude. At the highest TF ripple amplitude of $\delta_{BT} = 1.0\%$ the performance improvement due to the barrier is only slightly better that that of a plasma without an ITB ($\beta_N \approx 1.4$). Similar observations have been made for ITB scenarios with positive, zero or low magnetic shear [22].

2.2. EXPERIMENTS WITH DOMINANT ICRH

Instead of using the TF ripple to alter the rotation properties of the plasma, low torque experiments with a dominant fraction of ICRH have been carried out. Two issues may complicate such experiments; Firstly, the amount of ICRH power at JET is limited and the coupling is often compromised in the presence of ELMs. Secondly, coupling of ICRH on D or minority H ions, mainly heats the electrons, while the aim of this experiment is to study ion ITBs which may be governed by different physics than those in the electron channel. At JET an ITB scenario has been developed that uses ICRH coupling to ^{3}He minority and predominantly heats the ions, as long as the ^{3}He minority concentration, which is controlled in real-time, is kept below 8% [14]. At a magnetic

field of B = 3.45T (I_p = 2.5MA, q_{95} = 4.5), 37MHz ICRH provides central ion heating without coupling to other resonances. The high magnetic field also ensures a higher H-mode threshold and hence no or moderate ELMs, allowing good ICRH coupling up to 7MW. Similar to the scenario discussed in the previous section, a target q profile with reversed central magnetic shear is achieved by using a prelude of LHCD and early heating by NBI and ICRH. Figure 5 shows that ITBs are triggered, even with a large fraction of ICRH (69414) (P_{ICRH} = 6.1MW, P_{NBI} = 7.1MW) and low toroidal torque of 7.4Nm. The ρ^*_T contours and detailed analysis of the temperature time traces show that barriers are triggered at two times, the first, probably when q_{min} = 3 appears in the plasma and the second at q_{min} = 2. No MSE q profile measurements were available, but those from a similar discharge suggest that qρ2 and 3 surfaces appear just before these barriers form. The first barrier triggered in 69414 at t = 5.95s, shows the signs of a similar double-barrier structure as discussed in the previous section. At t = 8.0s a grand-cascade, likely to be caused by q_{min} = 2, is followed by the appearance of another small inner barrier. But both barriers in 69414 have little impact on the plasma performance and the ρ^*_T never reached above 0.021.

If this is compared with a scenario of identical plasma parameters, but dominant NBI heating, strong ITBs are seen to develop. Such a case, discharge 52881, is shown in figure 6. The main plasma parameters are the similar as for 69414 except for the heating scheme. The input power is similar, although, slightly higher (P_{NBI} = 12-13MW with P_{ICRH} = 3.7MW H minority heating) but the main difference with 69414 is the torque of about 13Nm. The barriers appear again at two times, presumably triggered again by the q = 3 and q = 2 surface appearing in the plasma, suggesting that the q profile characteristics are similar to those in 69414. The ITB reaches a peak strength of ρ^*_{Ti} = 0.045 (t = 10.4s). This plasma exhibits a significantly higher central rotation frequency of ~440km/s compared to ~85km/s for 69414 and consequently a much stronger gradient in the toroidal rotation when the ITBs are triggered, as can be seen in figure 7.

3. ITB GROWTH AND ROTATIONAL SHEAR
Rotational shear is thought to suppress turbulence, by affecting the growth and radial extent of turbulent eddies. Since the radial force balance equation indicates a connection between the radial electric field and cross field heat transport, toroidal momentum transport and poloidal rotation, there are various positive feedback mechanism possible [5]. Hence, the strengthening of a transport barrier may yield further suppression of turbulence by for example enhancing the rotational shear suggesting a non-linear growth until neo-classical transport levels are reached.

Detailed studies have shown that in JET negative magnetic shear may result in electron barriers by providing stabilisation of Trapped Electron Modes (TEMs) [25]. Similarly, various models were used to calculate the linear growth rate, γ, of for example Ion Temperature Gradient (ITG) driven turbulence, which is thought to be responsible for anomalous ion heat transport. However, the triggering of ion ITBs in JET are usually not predicted from transport models or turbulence simulations, i.e. overall rotational shear alone is not sufficient to trigger ITBs [25, 26].

The values of rotational shear or shearing rate $\omega_{E\times B}$ have been calculated using the JETTO code and compared with the ITG growth rate, as discussed in ref. [11, 25]. The shearing rate can be expressed as:

$$\omega_{E\times B} = \frac{RB_\theta}{B} \frac{\partial}{\partial r}\left(\frac{E_r}{RB_\theta}\right) \tag{1}$$

and the radial electric field, E_r, can be determined from the force balance equation:

$$E_r = v_\phi B_\theta - v_\theta B_\phi + \frac{1}{Zne} \frac{\partial P}{\partial r} \tag{2}$$

The radial electric field depends on the toroidal (f) and poloidal (q) components of the velocity, v, and magnetic field, B, and on the gradient of the pressure, P, (for a species with an atomic charge Z). Because a difference may exist between the rotation of the main ion species and that of Carbon, measured Carbon quantities have been used to determine the radial electric field. The poloidal rotation was assumed to be neo-classical and computed with the NCLASS code [24]. The JET plasmas, discussed here, are in the low collisionality regime and it has been demonstrated that in this case the dominant contribution to the rotational shear is usually the gradient in the toroidal rotation profile [11, 13]. These assumptions hold for plasmas without or with small barriers.

Figure 8 shows the calculated shearing rate at the time an ITB was triggered, for the four discharges with increasing TF ripple, shown in figure 4. The TF ripple change has clearly a strong effect on the rotational shear profiles. The strongest barriers are found to develop in discharges with a high shearing rate, such as 69670 which has $\omega_{E\times B} = 7\times10^4 s^{-1}$ near where the position of the ITB. Similarly, the discharge shown in figure 6 (51882) had a shearing rate of approximately $\omega_{E\times B} = 6\times10^4 s^{-1}$ at t = 9.93s, while its counter part with dominant ICRH heating (shown in figure 5) had a shearing rate as low as $\omega_{E\times B} = \sim1\times10^4 s^{-1}$ at the two times ITBs were triggered. The question is if these shearing rates are sufficient to stabilise turbulence. The values obtained above could be for example compared to a basic calculation of the ITG growth rate by JETTO. In those discharges that form strong ITBs, such as those shown in figure 1 (69670) and 5 (52881), the initial values were high and close to unity ($\omega_{ExB}/\gamma_{ITG} \sim 0.7$-$0.8$). High levels suggest a possible suppression of turbulence, although these calculations are rather basic and it is not accurately known what level $\omega_{ExB}/\gamma_{ITG}$ is required in order to cause turbulence stabilization.

A more accurate picture of the effect of the radial electric field or rotational shear on the turbulence growth rate can be obtained using gyro-kinetic simulations by the GYRO code [27, 28]. Linear and global modelling was performed using the Miller equilibrium, included kinetic electrons and collisions. All physical parameters were determined from experimental profiles. Only electrostatic fluctuations were included. For the case shown in figure 2 (with a TF ripple amplitude of $\delta_{BT} = 1.0\%$), the small rotational shear was found to have little effect on the physical growth rate of the modes, with $\gamma \sim 6\times10^4 s^{-1}$. This is still significantly larger than the shearing rate in this discharge.

6

However, for the case shown in figure 1 the physical growth rate was found to be reduced, although ITG modes were not completely suppressed, at the time of ITB triggering ($\gamma \sim 1.5 \times 10^4 s^{-1}$). Similarly, GLF23 modelling showed that rotational shear was still insufficient to suppress turbulence. Hence, the toroidal rotation and rotational shear was in neither of these cases responsible for the triggering of the ITB. But after the ITB triggering process, the growth of the barrier may enhance not only the temperature but also the toroidal rotation gradient, and is therefore able to further enhance the rotational shear. In figure 8, the level of rotational shear achieved during the maximum strength of the ITB in discharge 69670 is shown. GYRO calculations showed that at this time ITG modes were suppressed in the region of the transport barrier, albeit TEM modes were still present.

Besides the increase in toroidal rotation gradient, the assumption of neo-classical poloidal rotation may be invalid when the local temperature gradient length approaches the ion Larmor radius and this condition is reached in JET for strong ITBs. Poloidal rotation exceeding neo-classical values have been observed in JET plasmas with strong ITBs [29]. Figure 9 shows an example of rotation measurements with the JET Charge Exchange Spectroscopy (CXS) diagnostics. For the discharge 69670 (shown in figure 1), the poloidal and toroidal rotation profiles are shown, measured at the time the ITB triggers (t ~ 4.75s) and when the barrier is strongest (t ~ 5.75s). As expected the gradient in the toroidal rotation increases near the position of the barrier ($\rho \sim 0.6$) due to its effect on the momentum confinement further enhancing the toroidal component to the rotational shear. The poloidal rotation is, initially, close to the neo-classical values, however, when the ITB grows, it increases significantly. Poloidal rotation velocities 20 times the neo-classical value have been measured, peaking near the position of the barrier.

The enhanced poloidal rotation near the ITB region was found to have a large impact on the E×B shear and its component actually dominates over that of the toroidal rotation [30]. It could cause a 5 fold increase in shearing rate. As it seems that the amplitude of the poloidal rotation is linked to the strength of the barrier, its influence on the rotational shear is a non-linear component in the growth process. Hence, in plasmas with insufficient rotational shear to start with, a small 'seed-ITB', triggered by for example the specific characteristics of the q-profile, is not able to grow. In the other cases, however, the barrier may be able to push the sub-critical value $\omega_{ExB}/\gamma_{ITG}$ above unity, after which positive feedback is possible between the barrier strength, toroidal and poloidal rotational shear and stabilization of ITG driven turbulence, yielding a further growth of the barrier.

CONCLUSIONS

At JET the dynamics of Internal Transport Barriers (ITBs) has been explored by trying to decouple the effects of heating on one hand and torque. This was achieved by tuning the plasma rotation and rotational shear in scenarios that form ion ITBs, by tuning either the TF ripple or the fraction of ICRH to NBI power.

The experiments shed light on the physics behind the initial trigger for ion ITBs, which at JET often show to be linked to the shape of the q profile and magnetic shear. In JET the rotational shear

is usually found to be insufficient to trigger barriers, although it is well possible that this is the case in devices with a higher torque density. As described here, in plasmas with negative central shear and a low rotational shear, small, short-lived ion ITBs were triggered, which indicates that the overall rotational shear is not the dominant factor in this triggering mechanism. This does not mean that small scale changes in rotational shear or built-up of poloidal flow do not take part in this process. It shows that

ITBs may be triggered in plasmas with a low torque and low overall rotation such as in ITER. The subsequent growth of the internal transport barriers in JET, however, was affected by the rotational shear The high (above neo-classical) levels of poloidal rotation, measured during this phase, further strengthen this process. A 'seed-barrier', triggered by the appearance of a rational q surface in the plasma, may be able to kick-start this process, as long as sufficient initial rotational shear and momentum flux is available. Gyro-kinetic modelling showed that during this phase with a strong transport barriers, rotational shear affected the growth rate of turbulent modes. Only weak, transient ITBs were observed in discharges with a low torque and small rotational shear.

The improvement of transport in fusion plasmas is generally seen as a good thing, though the non-linear growth of the pressure gradient due to ITBs, may lead to unstable plasmas causing possibly a disruption of the discharge. Hence, control of the ITB growth should be understood. For the development of Advanced Tokamak scenarios the formation of wider, moderate but controllable barriers may be more favourable [31].

REFERENCES

[1]. Kikuchi, M, Nucl. Fusion **30** (1990) 265.

[2]. Litaudon, X., et al., Plasma Phys. Control. Fusion 44 (2002) 1057.

[3]. Luce, T.C., et al., Nucl. Fusion **43** (2003) 321.

[4]. Green, B.J., et al., Plasma Phys. Control. Fusion **45** (2003) 687.

[5]. Burrell, K.H., Phys. Plasmas **4** (1997) 1499.

[6]. Connor, J.W., et al., Nucl. Fusion **44** (2004) R1.

[7]. Challis, C.D., et al., Plasma Phys. Control. Fusion **43** (2001) 861.

[8]. Joffrin, E., et al., Nucl. Fusion **43** (2003) 1167.

[9]. Sakamoto, Y, et al., Nucl. Fusion **41** (2001) 865.

[10]. SYNAKOWSKI, E.J, et al., Phys. Rev, Lett. **78** (1997) 2972.

[11]. Tala, T., et al., Plasma Phys. Control. Fusion **43** (2001) 507.

[12]. Challis C. D. , et al., Plasma Phys. Control. Fusion **44** (2002) 1031.

[13]. De Vries, P.C., et al., Nucl. Fusion **48** (2008) 035007.

[14]. Hawkes, N.C., et al., "Ion Transport Barrier Formation with Low ExB Shear in JET", in Proc. of 34th EPS Conf. on Plasma Phys. Control. Fusion (Warsaw, 2007).

[15]. Sharapov, S.E., et al., Phys. Lett. A **289** (2001) 127.

[16]. Tresset, G., et al., Nucl. Fusion **42** (2002) 520.

[17]. Austin, M.E., et al., Phys. Plasmas, **13** (2006) 082502.

[18]. Romanelli, F, and Zonca, F, Phys. Fluids B **5** (1993) 4081.

[19]. Garbet, X, at al., Phys. Plasmas **8** (2001) 2793.

[20]. Waltz, R.E., et al., Phys. Plasmas **13** (2006) 052301.

[21]. Tubbing, B.J.D and the JET team, 'Experiments with TF ripple in JET', in the Proc. of the 22th EPS Conf. on Plasma Phys. Control. Fusion (Bournemouth, 1995) Vol. 19C, pIV-001 (1995).

[22]. De Vries, P.C., et al., Plasma Phys. Control. Fusion 50 (2008) 065008.

[23]. Shinohara, K, et. al., Nucl. Fusion 43 (2003) 586.

[24]. Houlberg, W., et al., Phys. Plasmas **4** (1997) 3231.

[25]. Baranov, Y.F., et al., Plasma Phys. Control. Fusion **46** (2004) 1181.

[26]. Tala, T., et al., Nucl. Fusion **46** (2006) 548.

[27]. Candy, J. and Waltz, R.E., J. Comput. Phys. **186** (2003) 545.

[28]. Candy, J. and Waltz, R.E., Phys. Rev. Lett. **2003** (2003) 045001.

[29]. Crombé, K., et al., Phys. Rev. Letters **95** (2005) 155003.

[30]. Crombé, K., et al., Plasma Phys. Control. Fusion 51 (2009) 055005

[31]. Rimini, F.G., et al., Fusion Energy 2008 (Proc. 22nd IAEA Conf., Geneva, 2008) IAEA Vienna, EX/1-2.
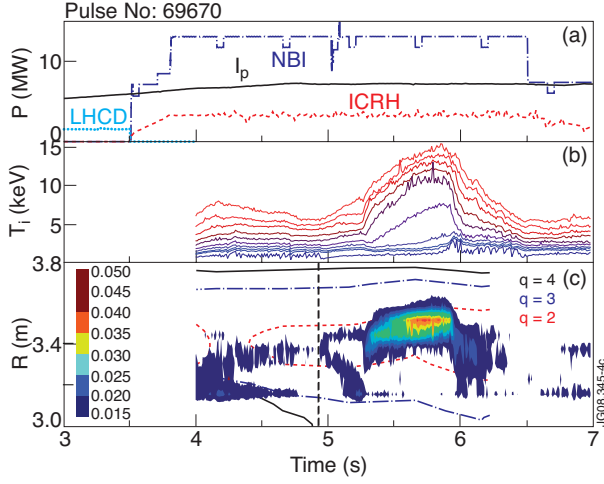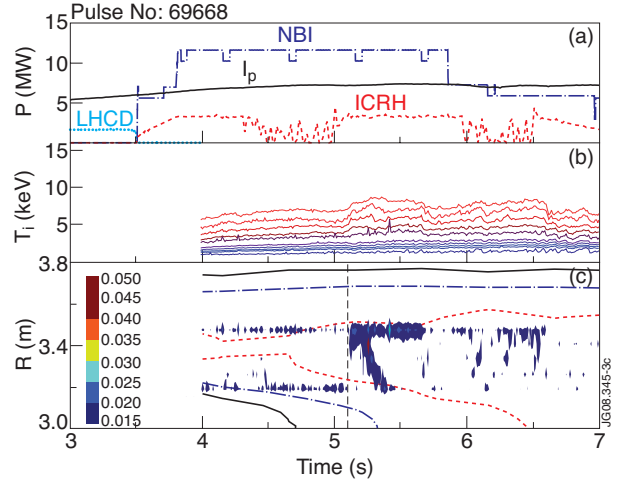
Figure 1: a) NBI, ICRH and LHCD powers and the plasma current, I_p, in arbitrary units, for discharges, 69670 (with a standard TF ripple of $\delta_{BT} = 0.08\%$) b) The ion temperatures measured at various radial locations (from the centre to the plasma edge). c) The integer value contours of the q-profile, overlaid with the contours of the ρ^*_{Ti}, with in blue the minimum level $\rho^*_T = \rho^*_T{}^{crit}$ and in red the maximum level ($\rho^*_T = 0.050$). The dashed lines give the time of the ITB trigger.

Figure 2: a) NBI, ICRH and LHCD powers and the plasma current, I_p, in arbitrary units, for discharges, 69668 (with a standard TF ripple of $\delta_{BT} = 1.0\%$) b) The ion temperatures measured at various radial locations (from the centre to the plasma edge). c) The integer value contours of the q-profile, overlaid with the contours of the ρ^*_{Ti}, with in blue the minimum level $\rho^*_T = \rho^*_T{}^{crit}$ and in red the maximum level ($\rho^*_T = 0.050$). The dashed lines give the time of the ITB trigger.
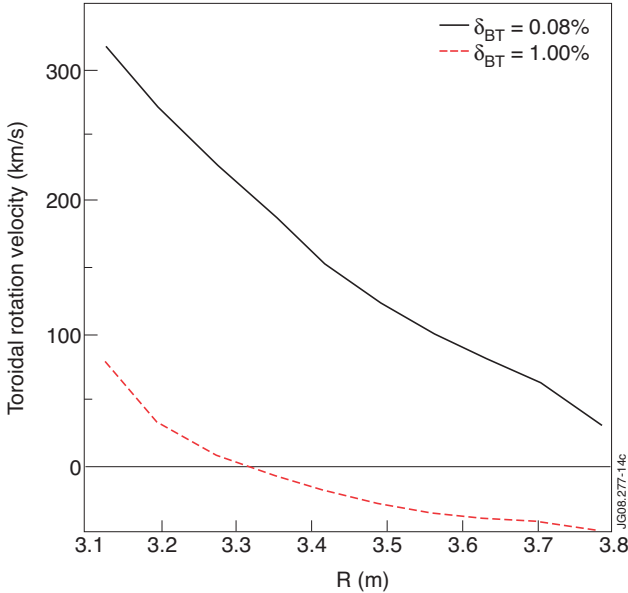
Figure 3: Toroidal rotation profiles measured at the time of ITB triggering for two discharges, with respectively, a small ($\delta_{BT} = 0.08\%$) and large TF ripple ($\delta_{BT} = 1.0\%$), respectively.
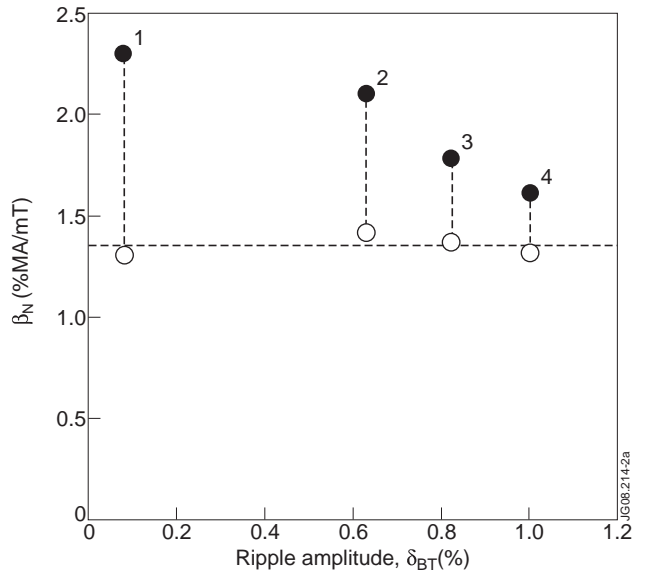
Figure 4: The performance expressed as β_N, as a function of TF ripple amplitude, δ_{BT}, for a series of discharges with reversed central magnetic shear. The open circles and dashed line give the value before the ITB development.
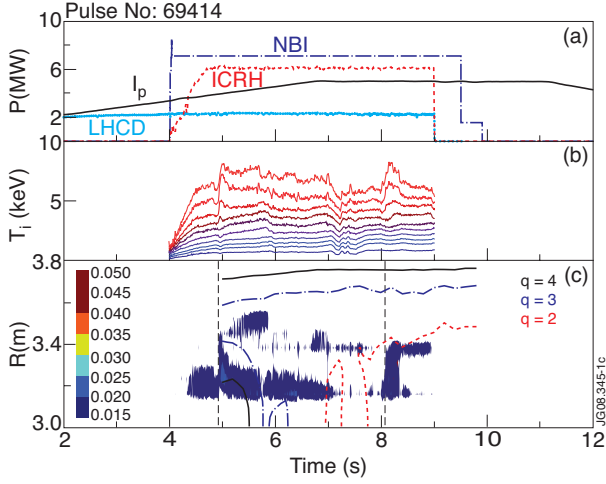
Figure 5: a) NBI, ICRH and LHCD power and the plasma current, I_p, in arbitrary units, for discharge, 69414 with a dominant fraction of ICRH (He^3 minority). b) The ion temperatures measured at various radial locations (from the centre to the plasma edge). c) The contours of the $\rho*_{Ti}$, with in blue the minimum level $\rho*_T = \rho*_T^{crit}$ and in red the maximum level (=$\rho*_T = 0.050$). In the left figure the q-profile contours for another, similar, discharge (69406) are shown for comparison. The dashed lines give the two times of the ITB triggering.
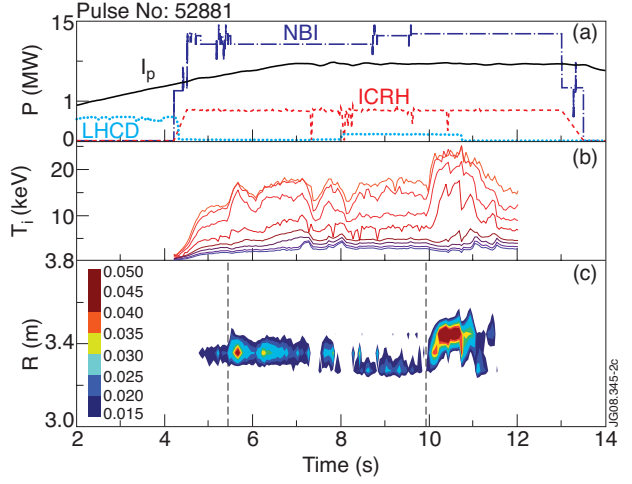
Figure 6: NBI, ICRH and LHCD power and the plasma current, I_p, in arbitrary units, for discharge 52881 with predominant NBI heating. b) The ion temperatures measured at various radial locations (from the centre to the plasma edge). c) The contours of the $\rho*_{Ti}$, with in blue the minimum level $\rho*_T = \rho*_T^{crit}$ and in red the maximum level (=$\rho*_T = 0.050$). The dashed lines give the two times of the ITB triggering.
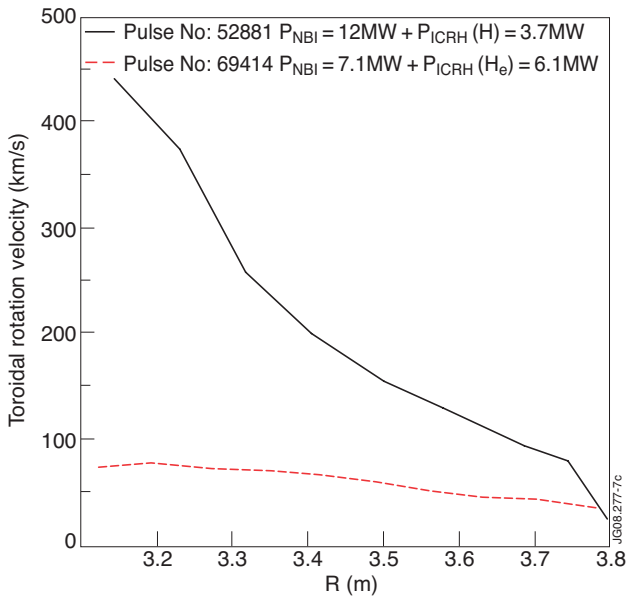

Figure 7: Toroidal rotation profiles measured at the time of ITB triggering for two discharges, shown in figure 5 and 6.
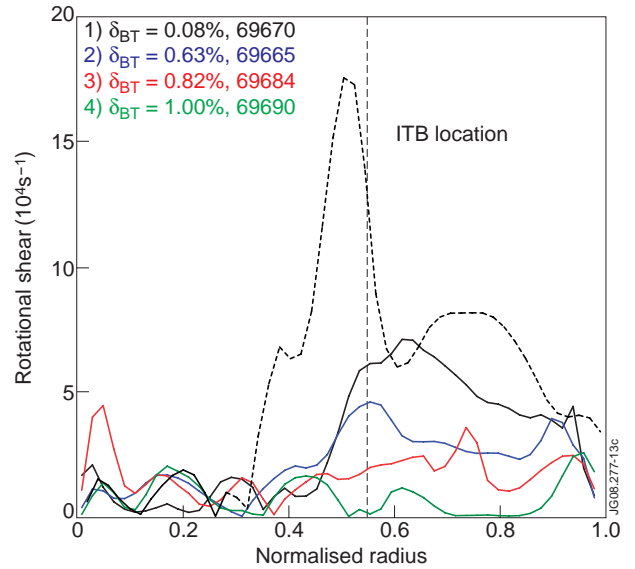
Figure 8: The rotational shearing rate profiles at the time the ITBs are triggered, for the discharges shown in figure 4 with various TF ripple amplitude (δ_{BT}). For discharge 69670, the profile at the time the ITB is strongest is shown (dashed curve). These profiles have been calculated under the assumption of neo-classical poloidal rotation. The dashed vertical line gives the approximate ITB position.
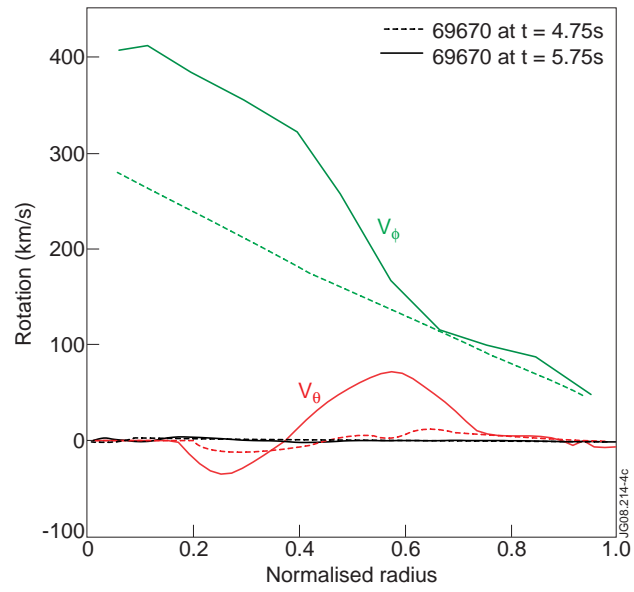
Figure 9: The change in the toroidal (green), V_ϕ, and poloidal (red), V_θ, rotation profiles, as measured by the JET CXS diagnostics, from just prior to the ITB trigger until it is at its maximum strength. The poloidal rotation predicted by NCLASS is shown in black.

12